NIH Public Access
Author Manuscript
J Allergy Clin Immunol. Author manuscript; available in PMC 2012 March 1.

Published in final edited form as:
J Allergy Clin Immunol. 2011 March ; 127(3): 773–786.e7. doi:10.1016/j.jaci.2010.10.018.

Tight Junction Defects in Atopic Dermatitis

Anna De Benedetto, MD[a], **Nicholas M. Rafaels, MS**[b], **Laura Y. McGirt, MD**[c], **Andrei I. Ivanov, PhD**[d], **Steve N. Georas, MD**[e], **Chris Cheadle, PhD**[b], **Alan E. Berger, PhD**[b], **Kunzhong Zhang, PhD**[f], **Sadasivan Vidyasagar, MD, PhD**[f], **Takeshi Yoshida, PhD**[a], **Mark Boguniewicz, MD**[g], **Tissa Hata, MD**[h], **Lynda C. Schneider, MD**[i], **Jon M. Hanifin, MD**[l], **Richard L. Gallo, MD**[h], **Natalija Novak, MD**[m], **Stephan Weidinger, MD**[n], **Terri H. Beaty, PhD**[o], **Donald Y. Leung, MD, PhD**[g], **Kathleen C. Barnes, PhD**[b], and **Lisa A. Beck, MD**[a]

[a] Department of Dermatology, University of Rochester Medical Center, Rochester, NY

[b] Lowe Family Genomics Core, Department of Medicine, Johns Hopkins University School of Medicine, Baltimore, MD

[c] Department of Dermatology, Johns Hopkins University School of Medicine, Baltimore, MD

[d] Department of Medicine, University of Rochester Medical Center, Rochester, NY

[e] Division of Pulmonary & Critical Care Medicine, University of Rochester Medical Center, Rochester, NY

[f] Radiation Oncology, University of Rochester Medical Center, Rochester, NY

[g] Department of Pediatrics, National Jewish Health, Denver, CO

[h] Division of Dermatology, University of California San Diego, San Diego, CA

[i] Division of Immunology, Children's Hospital Boston, Boston, MA

[l] Department of Dermatology, Oregon Health & Science University, Portland, OR

[m] Department of Dermatology and Allergy, University of Bonn (Germany)

[n] Department of Dermatology and Allergy, Technische Universität München (Germany)

[o] The Department of Epidemiology, Johns Hopkins Bloomberg School of Public Health, Baltimore, MD

Abstract

Background—Atopic dermatitis (AD) is characterized by dry skin and a hyperreactive immune response to allergens, two cardinal features that are caused in part by epidermal barrier defects. Tight junctions (TJ) reside immediately below the stratum corneum and regulate the selective permeability of the paracellular pathway.

Objective—We evaluated the expression/function of the TJ protein, claudin-1 in epithelium from AD and nonatopic (NA) subjects and screened two American populations for SNPs in *CLDN1*.

Corresponding Author: Lisa A. Beck, M.D., University of Rochester, Dept of Dermatology, 601 Elmwood Ave, Box 697, Rochester, NY 14642, Phone: 585-275-1039, Fax: 585-276-2330, Lisa_Beck@URMC.ROCHESTER.EDU.

Conflicts of Interest: None Declared

Publisher's Disclaimer: This is a PDF file of an unedited manuscript that has been accepted for publication. As a service to our customers we are providing this early version of the manuscript. The manuscript will undergo copyediting, typesetting, and review of the resulting proof before it is published in its final citable form. Please note that during the production process errors may be discovered which could affect the content, and all legal disclaimers that apply to the journal pertain.

NIH-PA Author Manuscript
NIH-PA Author Manuscript
NIH-PA Author Manuscript

NIH-PA Author Manuscript

NIH-PA Author Manuscript

NIH-PA Author Manuscript

Methods—Expression profiles of nonlesional epithelium from extrinsic AD, NA and psoriasis subjects were generated using Illumina's BeadChips. Dysregulated intercellular proteins were validated by tissue staining and qPCR. Bioelectric properties of epithelium were measured in Ussing chambers. Functional relevance of claudin-1 was assessed using a knockdown approach in primary human keratinocytes (PHK). Twenty seven haplotype-tagging SNPs in *CLDN1* were screened in two independent AD populations.

Results—We observed strikingly reduced expression of the TJ proteins claudin-1 and -23 only in AD, which were validated at the mRNA and protein levels. Claudin-1 expression inversely correlated with Th2 biomarkers. We observed a remarkable impairment of the bioelectric barrier function in AD epidermis. *In vitro*, we confirmed that silencing claudin-1 expression in human keratinocytes diminishes TJ function while enhancing keratinocyte proliferation. Finally, *CLDN1* haplotype-tagging single nucleotide polymorphisms revealed associations with AD in two North American populations.

Conclusion—Taken together, these data suggest that an impaired epidermal TJ is a novel feature of skin barrier dysfunction and immune dysregulation observed in AD, and that *CLDN1* may be a new susceptibility gene in this disease.

Keywords

atopic dermatitis; claudin-1; tight junctions

INTRODUCTION

Atopic Dermatitis (AD) is the most common inflammatory skin disease, affecting up to 17% of children and about 6% of adults in the US[1, 2]. Its cardinal features include dry, eczematous skin lesions, a relapsing and often chronic course and an intense, intractable pruritus. Many of these features have been attributed in part to an acquired and/or genetic epidermal barrier defect(s). Disturbance of the epithelial barrier is now recognized as a common feature in many inflammatory diseases including inflammatory bowel disease, celiac disease, sinusitis, food allergy, asthma, as well as AD[3, 4]. A defect in barrier has been argued to favor the penetration of microbes, allergens/antigens and irritants into the dermis, and possibly contribute to the Th2 immune response observed in early AD lesions[5–7].

The skin is the only epithelial surface that has two barrier structures: the stratum corneum (SC) and tight junctions (TJ)[8]. It is widely accepted in AD subjects that the SC is dysfunctional as the result of one or more of the following defects: 1) reduced levels of SC lipids[9–11], 2) acquired or genetic defects in filaggrin[12–14] or other epidermal differentiation proteins, 3) acquired or genetic defects in proteases and/or antiproteases[13, 15] and/or 4) simply the consequence of the physical trauma from widespread scratching that predates the development of all skin lesions.

TJ function as the "gate" for passage of water, ions and solutes through the paracellular pathway[16]. TJ also regulate the localization of apical and basolateral membrane components. Whether epidermal TJ have this cell polarity function is still debated[17]. Some investigators have speculated that TJ might regulate the lipid components found in the SC[18, 19]. This has promoted the notion that these two epidermal barrier structures interact in a dynamic way to ensure that the skin is in fact a formidable barrier. The structure and function of keratinocyte TJ remains an area of active investigation. TJ are composed of a number of transmembrane proteins such as the claudin family, junctional adhesion molecule (JAM)-A, occludin, and tricellulin. In addition, several scaffolding proteins such zonulae occludens (ZO)-1, ZO-2, ZO-3, multi-PDZ domain protein (MUPP)-1, membrane-associated guanylate kinase (MAGI) and cingulin have been identified in the TJ cytosolic

NIH-PA Author Manuscript

NIH-PA Author Manuscript

NIH-PA Author Manuscript

plaque[18]. Claudins are four-transmembrane-spanning proteins that determine TJ resistance and permeability and include over 24 members[20–22]. Based on *in vitro* experiments claudins have been divided into those that increase TEER or enhance barrier and include claudin-1 and -4, and claudins that reduce TEER and therefore disrupt barrier function, such as claudins-2 and -6[23].

Although, the existence of TJ-like structures in the epidermis has been suggested for some time[24], the functional relevance of these structures has been addressed only recently[21, 25, 26]. A major breakthrough came in 2002, when Furuse et al., reported that claudin-1-deficient mice died within 24 hr of birth with wrinkled skin, severe dehydration and increased epidermal permeability as measured by dye studies and transepidermal water loss (TEWL)[27]. Importantly, these mice had no abnormalities in the expression of stratum corneum proteins (e.g. loricrin, involucrin, transglutaminase-1 or Klf4) or lipids that might explain the severe skin phenotype. Although this mouse model clearly established the importance of claudin-1 in skin barrier function, very little is currently known about the role of claudin-1 (or TJ) in human skin diseases.

Dysfunction of keratinocyte TJ could explain many of the consequences of a defective skin barrier. For example, increased transepidermal water loss (TEWL), which is a well-established measure of skin barrier integrity and is notably elevated in both lesional and nonlesional skin of AD subjects, is still not readily attributable to *FLG* mutations[28–31]. Thus, other genetic or acquired defects in the skin barrier likely explain increased TEWL and the resulting dry skin that characterizes AD. Defective structure and function of TJ could also have immunological consequences. For example, Kubo et al. recently demonstrated that activated Langerhans cell, the resident antigen-presenting cell in the epidermis, gain access to foreign antigens by sending dendrites out through epidermal TJ[32]. It seems likely that Langerhans cell will be more likely to sample surface antigens and allergens when epidermal TJ are compromised. This coupled with the recent evidence that Langerhans cells are dendritic cells specialized to induce the differentiation of naive $CD4^+$ T cells to Th2 cells strongly supports the notion that a breach in TJ is likely a critical feature in the initiation of AD[33].

In the current study, we report for the first time the reduced expression of a key TJ protein, namely claudin-1 in AD epidermis which was not observed in subjects with psoriasis, a Th17-polarized inflammatory skin disease also associated with barrier defects[34, 35]. *In vitro* findings confirm that reductions in claudin-1 expression, comparable to that observed in human skin samples, significantly affect TJ function using two different measures of TJ integrity. Our *ex vivo* studies with full thickness epidermal samples demonstrate remarkable bioelectric defects in AD nonlesional skin and provide more insight into the mechanism of epidermal barrier dysfunction characteristic of AD. Preliminary SNP analysis, suggest that *CLDN1* may be a novel susceptibility gene for AD. Collectively, our studies strongly suggest that claudin-1 may be a key determinant of skin barrier dysfunction in AD, and may also be in part responsible for the Th2 polarization characteristically observed in the vast majority of cases.

METHODS

Study Participants – Expression Profiling and Validation Experiments

The diagnosis of AD was made using the US consensus conference criteria[36]. All AD subjects had extrinsic disease as defined by serum total IgE ≥ 2 SD of age-dependent norms and a positive multi-allergen RAST (ImmunoCap Phadiatop™). Non-atopic, healthy subjects (NA) were defined as having no personal or family history of atopic diseases, no personal history of chronic skin or systemic diseases and a serum total IgE that was ≤ 2 SD of age-

NIH-PA Author Manuscript

NIH-PA Author Manuscript

NIH-PA Author Manuscript

dependent norms and a negative Phadiatop™. The diagnosis of psoriasis was based on characteristic clinical features of plaque-type lesions by a board-certified dermatologist. Exclusion criteria were as follows: age ≤ 18 yrs, ≥ 60 yrs, use of systemic immunosuppressive therapy, leukotriene inhibitors within the last six weeks, use of topical steroids or calcineurin inhibitors within the last six weeks at the site of blister formation or biopsy, and subjects with a recent systemic infection or course of oral antibiotics within last two weeks. All subjects either underwent an epidermal procurement procedure (see below) or a 4 mm punch biopsy of their non-sunexposed forearm. These studies were approved by the Research Subject Review Boards at the Johns Hopkins Medical Institution and/or the University of Rochester Medical Center. All subjects gave written informed consent.

Epidermal Procurement and Processing

An NP-2 negative pressure vacuum apparatus (Electronic Diversities, Finksburg, Maryland, USA) was applied to the volar forearm (Figure 1B-D). The blister roof, which consists of full thickness epidermis, was removed using sterile technique and placed in Hank's Balanced Salt Solution (Invitrogen). Total RNA was extracted from epidermis using the QIAshredder spin column (Qiagen) and RNeasy RNA isolation kits (Qiagen). The quality of total RNA samples (RNA Integrity Number, RIN) was assessed using an Agilent 2100 Bioanalyzer (Agilent Technologies, Palo Alto, CA). Samples were selected for microarray analysis if they had a good RIN (range 8–10).

Gene Expression Profiling

Biotin-labeled, complementary RNA (cRNA) was prepared from total RNA according to manufacturer's protocol (Illumina, San Diego, CA). cRNA was hybridized to Illumina Sentrix HumanRef-8 Expression BeadChips (Illumina, San Diego, CA), which contain 24,350 probes corresponding to 21,429 unique genes. Signal intensity quantification was performed using an Illumina BeadStation 500GX Genetic Analysis Systems scanner.

Preliminary analysis of the scanned data was performed using Illumina BeadStudio software which returns single intensity data values for each probe following the computation of a trimmed mean average for each probe represented by a variable number of bead probes on the array. Z-transformation for normalization was performed on each Illumina sample/array on a stand-alone basis and Z ratios were calculated by taking the difference between the averages of the observed gene Z scores and dividing by the standard deviation of all the differences for that particular comparison[37]. Significant changes in gene expression between class pairs were calculated by Z test[38] and significant genes were defined as those which satisfy a Z test p-value of ± 1.5E-3. For Figure 4, the BeadStudio expression values for each sample/array were scaled to have median 256 and then $\log_2$ transformed.

Quantitative PCR (qPCR)

QPCR was performed using the iScript™ cDNA Synthesis kit and iQ™ SYBER Green Supermix assay system (Bio-Rad Laboratories). All PCR amplifications were carried out in triplicate on an iQ5 Multicolor real-time PCR detection system (Bio-Rad). Primers were designed and synthesized by Integrated DNA Technologies (Table E1 in the Online Repository). Relative gene expression was calculated by using the $2^{-\Delta\Delta Ct}$ method[39]. The normalized Ct value of each sample was calculated using GAPDH as an endogenous control gene.

Imaging of Tight Junction Proteins

For immunohistochemical staining the following Abs were used: claudin-1 (0.2 μg/ml, JAY. 8; Zymed), occludin (2.5 μg/ml, OC-3F10; Zymed), ZO-1 (2.5 μg/ml, ZO1-1A12; Zymed),

NIH-PA Author Manuscript

NIH-PA Author Manuscript

NIH-PA Author Manuscript

or isotype control. Five μm sections from formalin-fixed skin biopsies were deparaffinized and rehydrated. Slides were incubated in 1× EDTA solution, pH 8.0 at 95°C for 10min. Samples were incubated overnight at 4°C with primary Abs titered to the lowest concentration that produced immunoreactivity in control samples. The secondary antibodies and detection system used were reported previously[40]. For immunofluorescence labeling, skin samples were incubated in blocking solution (5% BSA, 0.1% saponin, 1mM calcium in PBS) for 20 min, followed by 90 min incubation with primary antibodies diluted in blocking solution. This was followed by a 1 h incubation with secondary antibodies; 1:1000 AlexaFluor 488 donkey-anti-rabbit IgG H+L (Molecular Probes), 1:1000Alexa Fluor 568 donkey-anti-mouse IgG H+L (Molecular Probes), 1:10,000 4′,6-diamidino-2-phenyl-indole, dihydrochloride (DAPI) (Molecular Probe). PHK grown on transwell filters or a glass coverglass were fixed in methanol at −20°C for 15 min, followed by blocking in PBS with 1% BSA and immunolabeled with the above TJ antibodies.

Flourescent images were obtained with an Olympus FV1000 laser scanning confocal microscope using the FV10-ASW 1.7 software. The Alexa Fluor 488 and 568 signals were imaged sequentially in frame interlace mode to eliminate crosstalk between channels. Saturation level of fluorescence intensity was set for the controls using the Hi-Lo feature of the Fluoview software. For each experiment, the images were captured at identical settings during image acquisition and no manipulations of the images occurred prior to importing into the FV1000 software at the workstation.

Ex vivo Electrophysiological Measurements in Ussing Chambers

Isolated blister roofs (1 cm in diameter; Figure 1B-D) were placed in the Ussing chamber in 2 mm diameter sliders for Snapwell chambers (area = 0.031 cm^2; Physiologic Instruments) and bathed in Ringer's lactate and gassed with a mixture of 95% O_2 and 5% CO_2. The tissues were continuously voltage-clamped to zero using VCC MC8 (Physiologic Instruments, San Diego, California, USA). Transepithelial short-circuit current (I_{sc}, expressed as μ•/cm^2 tissue surface area) were measured and total tissue conductance (G, expressed as mS/cm^2 tissue surface area) was calculated using Ohm's law by applying a 5 mV transepithelial pulse every 20 sec and measuring resulting current deflections.

Dilution potential measurements were performed to determine the changes in the permeability ratio between the Na^+ and Cl^- using the Nernst equation[41–43]. Briefly, the tissues were allowed to equilibrate in the Ussing chamber for 45 min. Ten nM bumetanide was added to both the apical/corneum and basolateral/basal bathing solutions to block Na^+-K^+-2Cl^- cotransport that feeds transepithelial Cl^- secretion via apical channels. Dilution potentials were induced by apical and/or basolateral perfusion with Ringer solutions containing two different concentrations of Na^+ (140 and 70 mM) and Cl^- (119.8 and 50 mM) and the remaining replaced with mannitol to maintain equal osmolarity between experiments. Dilution potentials were corrected for changes in junction potential (usually less than 1 mV). Change in membrane voltage (E_m) along with known concentrations of Na^+ and Cl^- in the respective solutions were substituted in the modified Nernst equation to determine the change in permeability ratio between Cl^- and Na^+ ($P_{Cl}[Cl]_i/P_{Na}[Na]_i$). $E_m=RT/F*2.303\log_{10}\{P_{Na}[Na]_o + P_{Cl}[Cl]_i/P_{Na}[Na]_i + P_{Cl}[Cl]_o\}$ R = 8.314472 (J/K/mol); F = 96.48531(KJ/mol); Permeability ratio (β) = P_{Cl} /P_{Na}; T = 310 (Kelvin).

Permeability Studies in Ussing Chambers

For the permeability assay 0.02% of FITC-albumin (Sigma) was added to the apical side of the inserts and buffer samples were collected at several time points (0.5 – 3 h) from the other side of the membrane. Permeability was assessed using a spectrophotometer (Multiskan EX;

NIH-PA Author Manuscript

NIH-PA Author Manuscript

NIH-PA Author Manuscript

Thermo Electron Corporation, Finland) at 490 nm. Permeability data were expressed as FITC fluorescence intensity normalized to sample area and time (O.D./cm^2/h).

Culture of Primary Human Foreskin Keratinocytes (PHK)

Human keratinocytes were isolated from neonatal foreskin[44]. PHK were cultured in Keratinocyte-SFM (Invitrogen/Gibco) with 1% Pen/Strep, 0.2% Amphotericin B (Invitrogen/Gibco). To differentiate PHK, cells were grown in DMEM (Invitrogen/Gibco) with 10% heat-inactivated fetal bovine serum (Invitrogen/Gibco) and 1% Pen/Strep, 0.2% Amphotericin B (Invitrogen/Gibco). For TJ modulation experiments, the following cytokines were added alone or in combination to the differentiation media; human IL-4 (50 ng/ml; R&D system) and IL-13 (50 ng/ml; R&D system).

Transepithelial Electric Resistance (TEER) and Paracellular Flux

PHK were plated at a subconfluent density of 2.5 – 3 $\times 10^4$ cells/filter in Transwell insert and cultured in Keratinocyte-SFM media until confluent. TEER was measured using an EVOMX voltohmmeter (World Precision Instruments, Sarasota, FL). The resistance of cell-free filters was subtracted from each experimental value.

To evaluate the paracellular flux of PHK, 0.02% Fluorescein (FITC) Sodium (Fluka) in HBSS was added to the upper chamber. Samples were collected from the lower chamber at different times (0.5 – 3 h). The amount of FITC that had diffused from the apical to the basal side of the filter was measured using a spectrofluorimeter (Multiskan EX; Thermo Electron Corporation, Finland) with excitation/emission wavelengths 490/514 nm. Paracellular permeability was presented as “Relative Fluorescence Flux” = Experimental condition/Filter alone × 100.

Immunoblotting

PHK were lysed on ice in RIPA lysis buffer (20 mM Tris, 50mM NaCl, 2mM EDTA, 2mM EGTA, 1% sodium deoxycholate, 1% TX-100, and 2% SDS, pH 7.4), with 1:100 Protease Inhibitor Cocktail (Sigma), 1:100 Phosphatase Inhibitor Cocktail (SigmaCells for 30 min at 4°C. The samples were heated at 95°C for 10 min and then centrifuged at 14,000rpm for 15 min. Forty μg of protein, determined by BCA (Pierce) in NuPage LDS Sample Buffer (Invitrogen) was applied to 4–12% NuPage Bis-Tris gels (Invitrogen). Electrophoresis was performed under reducing conditions with MES SDS Buffer (Invitrogen). Membranes were incubated in blotting solution (5% non-fat dry milk in PBS + 0.05% Tween 20) at RT for 1h and then incubated with primary antibodies; claudin-1 (JAY.8; Zymed), occludin (OC/3F10; Zymed) and GAPDH (FL-355; Santa Cruz). An HRP-linked secondary antibody (GE Healthcare) was used with ECL (GE Healthcare) to visualize bands by autoradiography with Kodak BioMax MR film. The pixel intensity of each band was estimated with Image J.

RNA Interference

PHK were plated on glass coverslips at 2 – 3 $\times 10^5$ cells/well in a 6-well plate or at 2 – 3 $\times 10^4$ cells/filter in Transwell insert (Costar; PET membrane, 0.4μm pore size, 6.5mm insert) in Keratinocyte-SFM without antibiotics. Next day after plating, cells were transfected with claudin-1 specific or control (scrambled) siRNAs (Santa Cruz) using Lipofectamine™ 2000 transfection Reagent (Invitrogen). TEER and permeability experiments were conducted 48 hours after PHK were switched to differentiation media.

Proliferation assay

To evaluate cell proliferation we used Click-iT EdU (5-ethynyl-29-deoxyuridine) kit following manufacturer’s instructions (Molecular Probes, Eugene, Ore). Cells were stained

NIH-PA Author Manuscript

NIH-PA Author Manuscript

NIH-PA Author Manuscript

with DAPI was to identify nuclei and assess cell density. For each sample, 6 random fields (magnification 3200) were captured. EdU positive cells were counted by 2 investigators blinded to the conditions, and results expressed as mean EdU positive cells/hpf.

Genetic Study Participants

DNA was isolated using standard protocols from 258 unrelated European American AD patients and 156 healthy controls participating in the ADVN. The same set of markers was genotyped on 176 African American AD patients, and 152 healthy controls. Baseline characteristics are presented in Table I and further details can be found in previous publications45. AD was diagnosed using the US consensus conference criteria[36]. Non-atopic, healthy controls were defined as having no personal history of chronic disease including atopy. AD severity was defined according to the 'eczema area and severity index' (EASI), a standardized grading system[46], and total serum IgE was measured. The study was approved by the institutional review boards at National Jewish Health, Johns Hopkins University, Oregon Health & Science University, University of California San Diego, Children's Hospital of Boston and University of Rochester Medical Center. All subjects gave written informed consent prior to participation.

Genotyping and Quality Control

We performed genotyping on genomic DNA extracted from blood samples using MagAttract DNA blood Mini M48 kit (QIAGEN) on a Biorobot M48, according to the manufacturer's instructions. DNA quantification was performed using Pico-Green (Pico-green, Molecular Probes). Genotyping in these samples was determined for each of the selected tagSNPs with the Illumina GoldenGate custom panel containing 384-plex assays according to the manufacturer's protocol (Illumina Inc., San Diego, CA).

Tagging SNPs were selected to represent the *CLDN1* gene in both the EA and AA groups. The SNP selection approach was to examine 10 kb upstream and 10 kb downstream in accordance with design score validations based on Illumina in-house measurements and the 60-bp limitation (a SNP cannot be closer than 60 bp to another SNP on this OPA). We initially selected all available *CLDN1* SNPs from the HapMap (http://www.hapmap.org/) to tag the linkage disequilibrium (LD) blocks in each of the ethnic groups (EA and AA). Tagging was based on the LDSelect algorithm47, 48, with a minor allele frequency (MAF) ≥10% and an r^2 threshold of 0.80 (as reported in HapMap) to ensure nearly perfect linkage disequilibrium (LD) in order to infer information on all SNPs captured by the tag set. A final selection included 27 SNPs chosen for the Illumina OPA. Of the 27 tagging SNPs selected, 24 qualified as tagging SNPs from both the HapMap CEPH Utah (CEU, with European ancestry) and the HapMap Yoruba (YRI, with African ancestry) samples; an additional three tagging SNPs (rs6800425, rs1155884, and rs9809713) were genotyped only in the AAs. Two LD blocks were observed among the European American group (block 1, rs10212165, rs3954259 and rs9290929 (D′ = 0.982–1.0); block 2, rs9835663 and rs3732923 (D′ = 0.976), and three LD blocks were observed among the African American group (block 1, rs3954259 and rs9290929 (D′ = 1.0); block 2, rs893051, rs9839711 and rs9835663 (D′ = 0.957–1.0); block 3, rs6800425 and rs3774028 (D′ = 1)) using the criteria of Gabriel et al[49].

The 27 SNPs were genotyped using the custom-designed Illumina oligonucleotide pool assay (OPA) for the BeadXpress Reader System and the GoldenGate Assay with VeraCode Bead technology (San Diego, CA, USA) according to the manufacturer's protocol[50]. Genotyping quality was high with an average completion rate of 97.2–98.2% for the BeadXpress genotyping. (see complete method in the Online Repository). All samples were also genotyped for the two FLG mutations most commonly associated with AD in EA (R501X and 2282del4), plus 9 additional polymorphisms (rs12730241, rs2065956,

NIH-PA Author Manuscript

NIH-PA Author Manuscript

NIH-PA Author Manuscript

rs11582620, rs3126082, rs6587665, rs11204980, rs1933063, rs1933064, rs3126091) as described[51]. Interaction among *FLG* mutations previously associated with AD as well as haplotype-tagging SNPs in *FLG* and *CLDN1* SNPs were investigated using PLINK epistasis. DNA samples from subjects enrolled for the immunostaining study were also genotyped for the same 2 *FLG* null mutations.

Statistical Analysis

Data were expressed as mean ± SEM of 3 or more experiments. Differences between groups were evaluated using an appropriate *t*-test. A *P* value of ≤ 0.05 was considered statistically significant. The statistical analysis performed as part of the expression profiling or SNP analyses are described in that section. The Cochran–Armitage trend test was used to test for association between each individual marker (under an additive model) and disease status using PLINK software (http://pngu.mgh.harford.edu/~purcell/plink/to). Analyses were performed for subjects of European and African ancestry separately to minimize confounding due to racial differences in polymorphism frequency. We tested for association between genetic markers and the quantitative measure of severity, EASI, using recessive logistic regression models. Departures from Hardy-Weinberg equilibrium (HWE) at each locus were tested by means of the chi-squared test separately for cases and controls using PLINK; all SNPs were in HWE. Tests for association that had a P value < 0.05 were then confirmed with PLINK max(T) test using 10,000 permutations.

RESULTS

Claudin-1 expression is markedly reduced in nonlesional AD epidermis

To characterize and quantify the expression of human epidermal proteins important for barrier function, we performed gene expression profiling of nonlesional or clinically unaffected epidermis using blister roofs from AD, PS, and NA subjects (Figure 1B-D). The Illumina Sentrix HumanRef-8 Chip contained 43 TJ genes (see Table E4 in the online Repository), 8 gap junction genes and 41 epidermal differentiation complex (EDC) genes. A number of the EDC genes were differentially expressed in AD versus NA nonlesional epidermis and several (e.g., S100A8, S100A7, FLG and LOR) (see Figure E1 in the Online Repository) corroborate the findings observed by others in lesional skin biopsies52, [53]. Of note FLG was down-regulated in AD vs NA (Z ratio: −5.29) however, the *P* value of 0.01 did not reach the significant threshold. Using the expression profiling array data from NA controls we verified that human keratinocytes express claudins-1, -4, -8, -12 and -1454–[56] and demonstrated for the first time that they also express claudins-15 and -23 (Illumina detection values ≥ 0.99; data not shown). Interestingly, of the intracellular junction genes, claudin-1 met our criteria for significance, demonstrating reduced expression in AD subjects with a Z ratio of −2.4 and *P* = 0.0013 compared to NA (Figure 1A – red highlights). We observed no difference in claudin-1 expression in psoriasis as compared to NA control subjects (*P* = 0.98) (Figure 1A – red highlights). We also noted reduced expression of claudin-23 (Z ratio: −3.2; *P* = 0.0062) in AD epithelium compared to NA but the difference was only marginally significant (Figure 1A – red highlights). Furthermore, AD subjects displayed enhanced expression of the gap junction proteins connexin-26 (*GJB2*, Z ratio: +5.2; *P* = 0.025) and connexin-62 (*GJA10*, Z ratio: +1.6; *P* = 0.001) (Figure 1A-red highlights). AD subjects did not show decreased expression of proteins relevant for adherens junctions or desmosomes (data not shown). Importantly, the expression of a number of differentiation genes were either not affected or increased in AD compared to controls (Figure 1A-Yellow highlighted genes) indicating that the observed changes in TJ genes did not simply reflect dedifferentiation of the epidermis. We confirmed the reduced expression of claudin-1 in blister roofs obtained from newly recruited AD and NA subjects (n = 5 per group) by qPCR (AD: 38.4 ± 7.1 RVU vs. NA: 69.7 ± 9.5; *P* = 0.03) (Figure 1E). We also

NIH-PA Author Manuscript

NIH-PA Author Manuscript

NIH-PA Author Manuscript

confirmed the reduced expression of claudin-23 (AD: 0.23 ± 0.04 RVU vs. NA: 0.81 ± 0.12; $P = 0.001$) and the enhanced expression of connexin-26 (GBJ2, AD: 18.87 ± 6.7 vs. NA: 3.73 ± 0.26; $P = 0.03$) in AD vs. NA controls by qPCR (Figure 1F). Although we considered the reduced expression of claudin-23 in AD samples very interesting, we were limited in our ability to pursue this interesting finding by the lack of good antibody reagents. Additional studies are clearly needed to clarify the role played by claudin-23 in epidermal barrier function.

In order to investigate claudin-1 expression in intact skin, we compared skin biopsies from nonlesional AD skin to NA using both immunohistochemistry (Figure 2A, B) and immunofluorescent/confocal microscopy (Figure 2C, D). Claudin-1 immunoreactivity was detectable in brightfield images in all suprabasal layers, while occludin and ZO-1 were detected only in the upper granulosum layer where TJ form (data not shown). This pattern as has been noted by other investigators [16, 57]. Importantly, the expression of claudin-1 was markedly reduced in nonlesional skin from subjects with AD compared to NA controls (Figure 2A-D). Semiquantitative claudin-1 scoring confirmed the markedly reduced staining (≥50%) in the epidermis of AD (1.3 ± 0.3) compared to NA subjects (2.9 ± 0.1; $P<0.0004$) and the highly significant P value demonstrates the remarkable uniformity of staining intensity within each group (Figure 2E). Immunofluorescent staining more clearly demonstrated claudin-1 immunoreactivity on the cell membranes. The signal intensity was again significantly less in AD samples (Figure 2C, D). These findings provide the first indication, to our knowledge, that the skin barrier defect in AD subjects may reside below the level of the SC, at the level of TJs.

AD epidermis shows defective bioelectric properties

We next investigated the functional impairment of TJ barrier in AD epidermis, by measuring bioelectric characteristics in Ussing chambers. This approach has been used in human and mouse models to evaluate the TJ bioelectric property of mucosal epithelia[58, 59]. The technique is based on the principle that an intact semi-permeable membrane will maintain the electrochemical potential gradient generated artificially by bathing each side of the epidermal sheets with solutions of different ionic strength[60, 61]. A leaky membrane will allow easy diffusion across the membrane and thus loss of electrochemical potential. Thus, the higher the permeability across a membrane the lower the potential gradient[59, 62]. TEERs were stable and typically quite high - indicating intact paracellular barrier function of the electrically active epithelium. Using this approach AD epidermis showed a dramatically lower resistance (92 ± 22.0 Ohms × cm^2; n = 3) as compared to NA subjects (827 ± 173.3 Ohms × cm^2; $P = 0.01$; n = 4) (Figure 3A). The lower resistance observed in the Ussing chambers was consistent with the increased permeability of FITC-conjugated albumin in AD (445 ± 24.25 O.D./cm^2/h; n = 3) as compared to NA samples (175 ± 68.37 O.D./cm^2/h; $P = 0.02$; n = 4) (Figure 3A). To better investigate the paracellular permeability properties we measured the relative permeability of Cl^- and Na^+ (P_{Cl}/P_{Na})[42]. If P_{Cl}/P_{Na} is equal to one then there is no selectivity and the membrane is freely permeable. Dilution potential studies on epidermal sheets showed the membrane selectivity is preserved in skin from NA subjects, with Na^+ ions relatively more permeable than Cl^- (0.77 ± 0.03 fold P_{Cl}/P_{Na}). However, in AD subjects' samples the selectivity was completely lost (1.1 ± 0.02 fold P_{Cl}/P_{Na}; $P = 0.001$; n = 3/group) as both ions were equally permeable (Figure 3B).

Claudin-1 expression inversely correlated with Th2 biomarkers

To address whether expression levels of epidermal claudin-1 might modulate adaptive immune responses we looked at the relationship between claudin-1 mRNA expression in our epidermal samples from AD, PS and NA controls and biomarkers of T helper (Th) 2 polarity namely, serum total IgE and peripheral blood eosinophilia (Figure 4A, B). Claudin-1 levels

NIH-PA Author Manuscript

NIH-PA Author Manuscript

NIH-PA Author Manuscript

were inversely correlated with both total IgE (r = − 0.718; *P* = 0.0038) and Eos (r = − 0.761; *P* = 0.0016) suggesting that reductions in this key TJ barrier protein may affect the character of the immune response to environmental allergens or vice versa.

Claudin-1 localizes to TJ only in differentiated human keratinocytes

Claudin-1 protein is expressed in primary human keratinocytes (PHK) *in vitro* but colocalizes with other TJ proteins at the cell membrane only after Ca^{+2}-induced differentiation (Figure 5A). Confocal microscopy demonstrated that claudin-1 colocalizes with occludin and ZO-1 at the areas of cell-cell contacts only in PHK grown in the media with high concentration of Ca^{+2} (Hi Ca; 1.9 mM) for at least 24h after confluency. Interestingly, in undifferentiated PHK grown in 0.3 mM Ca^{+2} (Lo Ca) containing media, claudin-1 immunoreactivity was faint and largely nuclear or perinuclear, while occludin was undetectable (Figure 5A) and ZO-1 localized on the membrane with a discontinuous pattern (data not shown).

Next we investigated the functional relevance of these Ca^{+2}-induced changes in TJ protein expression and localization. We observed during Ca^{+2}-induced PHK differentiation a dramatic (~300 fold) increase in TEER which peaked between 30 to 60h after exposure to high extracellular Ca^{+2} (Figure 5B), and confirmed previously published studies[27, 63–67]. Additionally, we showed that sodium fluorescein flux was markedly reduced in differentiated PHK (3.1 ± 0.6 fold; *P* = 0.046) (Figure 5C).

Th2 cytokines enhance claudin-1 expression and TJ barrier function

Previous studies have shown that claudin-1 expression in noncutaneous epithelial cells can be modulated by cytokines and growth factors[68–70]. Recent findings from mouse models support the hypothesis that IL-4 could delay skin barrier recovery[71, 72]. We therefore wondered if claudin-1 down-regulation observed in AD nonlesional skin biopsies could be secondary to Th2 cytokines. A corollary to this hypothesis is that even nonlesional skin has been shown to express Th2 cytokines[73]. To test this possibility, PHK were differentiated in the presence or absence of Th2 cytokines, IL-4 and IL-13 and the expression of claudin-1, occludin and ZO-1 was evaluated. We observed a significant enhancement of claudin-1 expression after IL-4 (48 hours, 50 ng/ml; 2.1 ± 0.4 fold over control; *P* = 0.05; n = 3) and IL-13 stimulation (48 hours, 50 ng/ml; 1.6 ± 0.3 fold over control; *P* = 0.1; n = 3; Figure 5D). No synergism was noted with both cytokines and interestingly we observed no effect on the expression of occludin and ZO-1 (data not shown). We then investigated the effect of IL-4 and IL-13 on PHK barrier function. A significant increase in TEER peak was observed in IL-4 (50 ng/ml) treated PHK (166 ± 24 Ohms × cm^2 vs media alone 109 ± 11 Ohms × cm^2; *P* = 0.03; n = 4). Dose response experiments confirmed IL-4's effect on TEER (dose range 0.5 – 100 ng/ml; data not shown). While, IL-13 (0.5 – 100 ng/ml) induced only a slight increase in TEER (data not shown). The mechanisms by which Th2 cytokines paradoxically enhance barrier function in our primary human keratinocytes is currently unknown, but these data suggest that the reduced claudin-1 expression and TJ dysfunction observed in AD subjects are not due to the actions of Th2 cytokines. Alternatively, we cannot rule out the possibility that AD epithelium would respond differently to Th2 cytokines and therefore studies are planned to address this possibility. Therefore at this point we cannot exclude the possibility that the impaired barrier observed in AD epidermis is a consequence of the Th2 cytokines present in the underlying dermis.

Claudin-1 knockdown disrupts TJ function and increased PHK proliferation

We utilized a RNA interference approach to evaluate the effect that claudin-1 reduction has on measures of TJ function (TEER and permeability) and proliferation. Figure 6A shows that claudin-1-specific small interfering (si)RNA induced a dose-dependent and significant

NIH-PA Author Manuscript

NIH-PA Author Manuscript

NIH-PA Author Manuscript

(≤60%) decrease in protein expression compared to scrambled siRNA-transfected cells. Since the claudin-1 KO mouse dies shortly after birth and our tissue staining demonstrated ~50% reduction in claudin-1 immunoreactivity in AD compared to NA epithelium (Figure 2), we chose to perform our functional assessments with a dose of siRNA (100 nM) that reduced claudin-1 transcripts by a similar amount ($P = 0.01$). With only a 50% reduction in claudin-1, TEER dropped by ≥50% (Figure 6C) (control: 164 ± 18.2 and CLDN1 siRNA: 80.6 ± 6.4 ohms × cm^2; $P = 0.007$; n = 4) and permeability to sodium fluorescein increased by a similar extent (Figure 6D) (control: 27.6 ± 11.7 and CLDN1 siRNA: 52.5 ± 9.2; $P = 0.026$; n = 4) when compared to the scrambled siRNA-transfected PHK. Yamamoto et al. used a similar knockdown strategy but observed a more modest effect (14% reduction) on TEER and did not assess TJ function using a permeability assay[63]. We also investigated the effect of claudin-1 knockdown on connexin-26 (*GJB2*), since this was upregulated in AD array samples. We observed enhanced expression of connexin-26 in our knockdowns (1.7 ± 0.8 fold over control; $P = 0.05$; n = 6; Figure E2 in the Online Repository).

Using a proliferation assay based on EdU incorporation, we noted that claudin-1 depleted cells have more proliferating cells (21.6 ± 1.4 EdU positive cells/hpf) compared to control (8.1 ± 2 EdU positive cells/hpf; $P = 0.002$; n = 3) (Figure 6E).. These studies confirm and extend (with permeability and proliferation assays) previously published studies[27, 63–67] which, have implicated claudin-1 as a critical protein for the establishment of a functional paracellular epidermal barrier. The proliferation we observed in claudin-1 knockdowns suggest that this may be responsible for the enhanced epithelial thickness or acanthosis observed in nonlesional AD skin.

CLDN1 variants are associated with risk of AD

Because our findings strongly implicated claudin-1 as a critical element in risk of AD, we took advantage of the ongoing NIAID-funded Atopic Dermatitis and Vaccinia Network (ADVN), which is currently enrolling subjects with AD and NA (reviewed in a previous publication45), to examine whether common variants in the human *CLDN1* gene might be associated with susceptibility to AD and disease severity. Two independent groups (European American, African American) of AD patients and healthy controls were enrolled (Table I). In brief, AD was diagnosed using the US consensus conference criteria36, and AD severity was defined according to the 'eczema area and severity index' (EASI), a standardized grading system46. Twenty-seven *CLDN1* SNPs spanning a 31.5 kb region on chromosome 3q28-q29 were selected using a haplotype-tagging approach, of which 24 were common to both ethnic groups (see Table E2 in the Online Repository). Adjusting for 10,000 permutations, we observed the most significant associations for a lower risk of AD in the African American group for an intronic SNP (rs17501010) between the 3rd and 4th exons of *CLDN1* ([OR], 0.5, 95% CI = 0.3–0.8; $P = 0.003$) and an adjacent SNP (rs9290927) downstream of rs17501010 that was associated with a higher risk of AD ([OR], 1.8, 95% CI = 1.0–3.3; $P = 0.004$) (Figure 7 and Table E3 in the Online Repository). SNP-rs17501010 also showed a modest association with early onset AD (<5 yrs of age- $P = 0.04$). In addition, two SNPs (rs893051 in intron 1 and rs9290929 in the promoter region) were associated with greater disease severity ([OR], 1.5, 95% CI = 1.1–2.1 $P = 0.010$; 1.6, 95% CI = 1.1–2.3 $P = 0.007$, respectively; Figure 7 and Table E3 in the Online Repository). Modest associations were observed in the European American group, including a promoter SNP (rs16865373) and lower risk of AD ([OR], 0.5, 95% CI = 0.2–0.9; $P = 0.034$) and lower risk of early onset AD (<5 yrs of age - [OR], 0.4, 95% CI = 0.2–1.0; $P = 0.034$; Figure 7 and Table E3 in the Online Repository). Haplotype analyses were performed but did not alter the evidence for association for any of the outcomes, including FLG null mutation (e.g., R501X and 2282del4) phenotype (data not shown). Considering the importance of *FLG* mutations in AD and its subphenotypes, we also evaluated whether there was an interaction between

NIH-PA Author Manuscript

NIH-PA Author Manuscript

NIH-PA Author Manuscript

haplotype-tagging SNPs in *FLG* and *CLDN1*. No significant interaction effect was found. Despite the limitations of relatively small sample sizes, these findings suggest that *CLDN1* genetic variations may determine risk for and severity of AD in ethnically diverse populations and that this appears to be independent of *FLG*.

DISCUSSION

This is the first report, to our knowledge, implicating a TJ defect in AD, a human skin disease that affects up to 15 million Americans. We demonstrated reduced expression of epidermal claudin-1 in AD nonlesional epidermis (Figure 2). This was specific for AD and not observed in psoriasis, a Th17-driven inflammatory skin disorder (Figure 1). Although previous psoriasis publications have suggested that TJ may be altered in lesional epidermis this has not been consistently observed by other groups[56, 74–76]. Adapting the Ussing chamber to measure bioelectric properties of stratified squamous epithelium enabled us to characterize skin barrier properties from human subjects. Using this approach we observed a remarkable alteration in the bioelectric characteristics of AD epidermis with markedly lower electrical resistance and higher albumin permeability that was associated with the loss of ion selectivity permeability (Figure 3). These defects are the signature of a TJ defect.

Our findings are highly consistent with the observations made from genetically altered mice. For example, the claudin-1 knockout mouse dies within 24 hr of birth with wrinkled skin, severe dehydration and increased epidermal permeability as measured by dye studies and TEWL[27]. Importantly, these mice have no abnormalities in the expression of stratum corneum proteins (e.g., loricrin, involucrin, transglutaminase-1, or Klf4) or lipids that might explain their severe skin phenotype. Another recent study reported disruption of epidermal barrier and severe dermatitis in transgenic mice overexpressing an adhesion-deficient mutant of claudin-6 in the suprabasal compartment of the skin[77]. Interestingly, a marked downregulation of claudin-1 expression was noted in these transgenic mice. It is tempting to speculate that the reduction in claudin-1 rather than the adhesion-defective claudin-6 per se was responsible for the barrier disruption observed in this mouse. Lopardo et al. also observed reduced claudin-1 expression in the epidermis of p63 mutant mice66. These mice have a severe skin phenotype and die of dehydration within one day of birth similar to the claudin-1 KO mice. In summary, these mouse models have highlighted the critical importance of claudin-1 for a functional epidermal TJ. Recently, a human syndrome caused by an exonic mutation in the *CLDN1* has been described78–[80]. Patients with this syndrome called Neonatal Ichthyosis-Sclerosing Cholangitis (NISCH) have features in common with AD, namely erythema, dry flaky skin and patchy alopecia in addition to unique features such as severe liver and gallbladder abnormalities that likely arise because of the importance of claudin-1 in the barrier integrity of bile canaliculi[78, 79].

Our *in vitro* studies with PHK monolayers demonstrating a clear association between claudin-1 levels and TEER confirmed previous work[55, 57, 63, 81, 82]. We extended these findings by demonstrating that claudin-1 knockdown also enhanced TJ permeability and proliferation (Figure 6). In our study, the claudin-1 siRNA was target-specific, with no changes observed in the expression and/or localization of other critical TJ proteins (occludin and ZO-1), adherens junction components (E-cadherin and nectin-1) or stratum corneum proteins (filaggrin) (Figure E2). Additionally, we were able to reduce claudin-1 expression by ~50% - similar to the reductions we observed in claudin-1 immunoreactivity of AD epidermis and this resulted in a remarkable reduction (~50%) in TJ function (based on both electrical resistance and permeability assays) (Figure 6). While immunolabeling data allow only a correlative link between claudin-1 expression and the development of epidermal barrier, our RNA interference result demonstrated a causal connection between these two events (Figure 6).

NIH-PA Author Manuscript

NIH-PA Author Manuscript

NIH-PA Author Manuscript

Recent studies with different types of mammalian epithelia indicated that the epithelial barrier is determined by two different components, charge-selective small pores that are permeable to molecules with up to 4μ radius, and large, poorly-defined breaks of the barrier without size- or charge-selectivity (reviewed in83). TEER reflects small-pore permeability, whereas flux of FITC with a reported Stokes' radius of ~5.5• measures permeability of large barrier breaks. Knockdown of claudin-1 in PHK monolayers decreased TEER and increased FITC flux, which implicates claudin-1 in regulation of both paracellular pores and breaks in the epidermal barrier. These findings strongly suggest that the skin of AD subjects would also be more permissive to a number of relevant environmental allergens such as house dust mite. Purified allergens from the house dust mite, *Dermatophagoides pteronyssinus* have a diameter of ~1.6• by X-ray crystallography and therefore could penetrate even small paracellular pores formed by epithelial TJs[84]. Thus, defective expression and function of claudin-1 in AD provides a plausible molecular mechanism for increased sensitization to environmental antigens, allergens, irritants, or pollutants. This is in keeping with the distinction that AD is the allergic disorder with the greatest and most diverse allergen reactivity, reflected in high serum total IgE values. AD is also recognized for a reduced cutaneous irritancy threshold that could simply reflect greater epidermal penetration of irritants. Importantly, TJ disruption is a leading hypothesis to explain allergen reactivity in the airways, which manifests as asthma and allergic rhinitis or in the intestinal tract as food allergy[3, 85, 86].

Although we observed an inverse correlation between claudin-1 expression and markers of Th2 polarity we did not find that Th2 cytokines (IL-4 and IL-13 alone or together) reduced claudin-1 expression but in fact observed the opposite. This induction of claudin-1 was observed in conjunction with enhanced TJ function (e.g. TEER) and suggests that Th2 cytokines have a reparative effect on TJ in normal keratinocytes. Whether the actions of these Th2 cytokines would be different in AD epidermis will require further study. Interestingly Th2 cytokines have been shown to reduce the expression of several SC components important for skin barrier function[72]. At this point we conclude that TJ dysfunction observed in AD epidermis is not likely caused by Th2 milieu, which is present even at nonlesional sites. Instead we would hypothesize that the connection we observed between TJ function and biomarkers of Th2 polarity suggest that AD TJ defects enable or promote Th2 responses possibly by enhancing the trafficking of non-self antigens that are responsible for triggering the Th2 response in genetically predisposed individuals. Alternatively, the upregulation of claudin-1 in response to IL-4 and IL-13 may represent a compensatory immune response to "protect" against further antigen uptake through the skin.

In preliminary studies we evaluated genetic associations between *CLDN1* polymorphisms and AD. We undertook a haplotype-tagging SNP approach using genetic markers available in the public arena (n = 132 in dbSNP) in 414 European Americans and 328 African Americans. Interestingly, *CLDN1* is localized on chromosome 3q28–q29, very close to the *ATOD1* locus for AD[90]. Adjusting for 10,000 permutations to reduce a Type I error due to multiple comparisons, we observed several modest associations (P = 0.003 – 0.05) between variants throughout the *CLDN1* gene and the outcomes associated with AD, especially among African American patients. In separate studies we tested for association between several of the same *CLDN1* SNPs and risk of disease among a more robustly powered German dataset of AD patients and controls; however, the full set of SNPs genotyped in the ADVN study were not available for direct comparisons, and phenotyping approaches differed (data not shown). Further studies are underway for comprehensive joint analyses between ADVN and the German study. Interestingly, *CLDN1* variants were also associated with asthma and its related trait, total serum IgE and FEV_1, in two independent populations of African descent (K. Barnes unpublished data). In addition, the rs893051 SNP associated with AD severity in our AA population, was also associated with asthma and disease

NIH-PA Author Manuscript

NIH-PA Author Manuscript

NIH-PA Author Manuscript

severity in a population of African descent. As part of the ADVN study our population was also screened for the two most frequent *FLG* mutations (R501X and 2282del4; Table I) and 9 haplotype-tagging SNPs throughtout the *FLG* gene[51]. There were no significant interaction effects between haplotype-tagging SNPs in *FLG* and *CLDN1* SNPs. Moreover, in the AA population where we had the strongest association with *CLDN1* SNP*s*, the 2 *FLG* mutations were considerable less common than in our EA population[51]. Our findings provide suggestive evidence for a role of *CLDN1* variants in AD and its associated phenotypes, further supporting the importance of *CLDN1* in AD. In conclusion, this study provides the first evidence that epidermal TJs are defective in AD, the most common human skin disease. We observed that claudin-1 is selectively reduced in the epidermis of AD patients and that *CLDN1* may be a novel AD susceptibility gene. Epidermal samples from AD subjects had remarkable defects in resistance and ion transport compared to healthy controls. Using the model of human keratinocyte monolayers, we observed enhanced claudin-1 expression and recruitment to intercellular junctions, upon cell differentiation, which coincided with the development of a paracellular barrier. Selective downregulation of claudin-1 expression markedly increased paracellular permeability, decreased resistance and enhanced proliferation indicative of a wound repair response. We hypothesize that the reduced expression of claudin-1 in AD epidermis may enhance the penetration of many relevant environmental antigens leading to greater allergen sensitization as well as greater susceptibility to irritants/pollutants and possibly even altered microbial flora. The inverse relationship between claudin-1 and serum total IgE values also suggests that this defect may promote Th2 responses. Collectively this data suggests that barrier dysfunction in subjects with AD extends beyond the stratum corneum to TJ the second barrier structure and that barrier regulation provides a novel therapeutic opportunity in AD and possibly other atopic disorders.

Key Messages

- Claudin-1 plays a critical role in human epidermal tight junction function and keratinocyte proliferation.
- Claudin-1 is significantly reduced in nonlesional skin of AD compared to NA and psoriasis subjects.
- Claudin-1 levels are inversely correlated with Th2 biomarkers suggesting that reductions in this key TJ barrier protein may affect the character of the immune response to environmental allergens.
- Analysis of claudin-1 (*CLDN1*) haplotype-tagging single nucleotide polymorphisms in two North American populations revealed associations with AD.

Supplementary Material

Refer to Web version on PubMed Central for supplementary material.

Acknowledgments

We would like to acknowledge Mark Slifka, PhD at Oregon Health & Science University (Beaverton, OR) for careful review of the manuscript and helpful suggestions. Dr. Rasika Mathias for advice on interpretation of SNP findings. Mary Brummet, MS at the Johns Hopkins Asthma & Allergy Center (Baltimore, MD) and Mary Bolognino, BS at the University of Rochester Medical Center (Rochester, NY) for facilitating experiments and providing us with PHK. We would also like to acknowledge several groups whose efforts made the clinical enrollment possible: ADVN Coordinators (Patricia Taylor, NP; Trista Berry, BS; Susan Tofte, FNP; Shahana Baig-Lewis, MPH; Peter Brown, BS; Lisa Heughan, BA, CCRC; Meggie Nguyen, BS; Doru Alexandrescu, MD; Lorianne Stubbs, RC; Reena Vaid MD; Diana Lee, MD), ADVN regulatory advisors (Judy Lairsmith, RN and Lisa

NIH-PA Author Manuscript

NIH-PA Author Manuscript

NIH-PA Author Manuscript

Leventhal, MSS, CIM, CIP), biological sample tracking (JHU - Tracey Hand, MSc; Jessica Scarpola, and Muralidhar Bopparaju, MSc, and URMC - Mary Bolognino, MS), NIAID-DAIT oversight (Marshall Plaut, MD and Joy Laurienzo Panza, RN, BSN), DACI Laboratory (Robert Hamilton, PhD), Rho®, Inc. statistical support (Daniel Zaccaro, MS and Brian Armstrong, MPH) Rho®, Inc. general study support and oversight (Jamie Reese, BS; Susi Lieff, PhD; and Gloria David, PhD, MHSc) and last but by no means least, all the patients who participated in this study.

Funding: The Atopic Dermatitis and Vaccinia Network NIH/NIAID (contract N01 AI40029 and N01 AI40033), National Eczema Association (A.D.), Mary Beryl Patch Turnbull Scholar Program (K.C.B.).

Abbreviations

AA	African American
AD	Atopic Dermatitis
ADVN	Atopic Dermatitis and Vaccinia Network
CLDN1	Claudin 1
CLDN23	Claudin 23
EA	European American
EASI	Eczema Area and Severity Index
IVL	involucrin
I_{sc}	Transepithelial short-circuit current
LD	Linkage Disequilibrium
MAF	Minor Allele Frequency
MOI	Multiplicity of Infection
NA	Nonatopic
OCLN	occluding
PPL	periplakin
PHK	Primary Human Foreskin Keratinocytes
qPCR	Quantitative PCR (e.g., Real-time PCR)
RIN	RNA Integrity Number
RVU	Relative Value Units
SNP	Single Nucleotide Polymorphism
SPRR	small proline rich proteins
SC	Stratum Corneum
TJ	Tight Junctions
TEER	Trans Epithelial Electrical Resistance
TGM1	transglutaminase 1
TEWL	Transepithelial Water Loss
UTR	Untranslated Region
ZO	Zonulae Occludens

NIH-PA Author Manuscript

NIH-PA Author Manuscript

NIH-PA Author Manuscript

References

1. Laughter D, Istvan JA, Tofte SJ, Hanifin JM. The prevalence of atopic dermatitis in Oregon schoolchildren. J Am Acad Dermatol 2000;43:649–55. [PubMed: 11004621]
2. Odhiambo JA, Williams HC, Clayton TO, Robertson CF, Asher MI. Global variations in prevalence of eczema symptoms in children from ISAAC Phase Three. J Allergy Clin Immunol 2009;124:1251–8. e23. [PubMed: 20004783]
3. Schulzke JD, Ploeger S, Amasheh M, Fromm A, Zeissig S, Troeger H, et al. Epithelial tight junctions in intestinal inflammation. Ann N Y Acad Sci 2009;1165:294–300. [PubMed: 19538319]
4. Holgate ST. Epithelium dysfunction in asthma. J Allergy Clin Immunol 2007;120:1233–44. quiz 45–6. [PubMed: 18073119]
5. Demehri S, Morimoto M, Holtzman MJ, Kopan R. Skin-derived TSLP triggers progression from epidermal-barrier defects to asthma. PLoS Biol 2009;7:e1000067. [PubMed: 19557146]
6. Holgate ST. The epithelium takes centre stage in asthma and atopic dermatitis. Trends Immunol 2007;28:248–51. [PubMed: 17466594]
7. Hata M, Tokura Y, Takigawa M, Sato M, Shioya Y, Fujikura Y, et al. Assessment of epidermal barrier function by photoacoustic spectrometry in relation to its importance in the pathogenesis of atopic dermatitis. Lab Invest 2002;82:1451–61. [PubMed: 12429806]
8. Madison KC. Barrier function of the skin: ''la raison d'etre'' of the epidermis. J Invest Dermatol 2003;121:231–41. [PubMed: 12880413]
9. Imokawa G. Lipid abnormalities in atopic dermatitis. J Am Acad Dermatol 2001;45:S29–32. [PubMed: 11423869]
10. Murata Y, Ogata J, Higaki Y, Kawashima M, Yada Y, Higuchi K, et al. Abnormal expression of sphingomyelin acylase in atopic dermatitis: an etiologic factor for ceramide deficiency? J Invest Dermatol 1996;106:1242–9. [PubMed: 8752664]
11. Pilgram GS, Vissers DC, van der Meulen H, Pavel S, Lavrijsen SP, Bouwstra JA, et al. Aberrant lipid organization in stratum corneum of patients with atopic dermatitis and lamellar ichthyosis. J Invest Dermatol 2001;117:710–7. [PubMed: 11564181]
12. Palmer CN, Irvine AD, Terron-Kwiatkowski A, Zhao Y, Liao H, Lee SP, et al. Common loss-of-function variants of the epidermal barrier protein filaggrin are a major predisposing factor for atopic dermatitis. Nat Genet 2006;38:441–6. [PubMed: 16550169]
13. Cork MJ, Robinson DA, Vasilopoulos Y, Ferguson A, Moustafa M, MacGowan A, et al. New perspectives on epidermal barrier dysfunction in atopic dermatitis: gene-environment interactions. J Allergy Clin Immunol 2006;118:3–21. quiz 2–3. [PubMed: 16815133]
14. Howell MD, Kim BE, Gao P, Grant AV, Boguniewicz M, DeBenedetto A, et al. Cytokine modulation of atopic dermatitis filaggrin skin expression. J Allergy Clin Immunol 2009;124:R7–R12. [PubMed: 19720210]
15. Vasilopoulos Y, Cork MJ, Teare D, Marinou I, Ward SJ, Duff GW, et al. A nonsynonymous substitution of cystatin A, a cysteine protease inhibitor of house dust mite protease, leads to decreased mRNA stability and shows a significant association with atopic dermatitis. Allergy 2007;62:514–9. [PubMed: 17441792]
16. Schluter H, Moll I, Wolburg H, Franke WW. The different structures containing tight junction proteins in epidermal and other stratified epithelial cells, including squamous cell metaplasia. Eur J Cell Biol. 2007
17. Umeda K, Ikenouchi J, Katahira-Tayama S, Furuse K, Sasaki H, Nakayama M, et al. ZO-1 and ZO-2 independently determine where claudins are polymerized in tight-junction strand formation. Cell 2006;126:741–54. [PubMed: 16923393]
18. Niessen CM. Tight junctions/adherens junctions: basic structure and function. J Invest Dermatol 2007;127:2525–32. [PubMed: 17934504]
19. Leyvraz C, Charles RP, Rubera I, Guitard M, Rotman S, Breiden B, et al. The epidermal barrier function is dependent on the serine protease CAP1/Prss8. J Cell Biol 2005;170:487–96. [PubMed: 16061697]
20. Tsukita S, Furuse M, Itoh M. Multifunctional strands in tight junctions. Nat Rev Mol Cell Biol 2001;2:285–93. [PubMed: 11283726]

NIH-PA Author Manuscript NIH-PA Author Manuscript NIH-PA Author Manuscript

21. Tsukita S, Furuse M. Claudin-based barrier in simple and stratified cellular sheets. Curr Opin Cell Biol 2002;14:531–6. [PubMed: 12231346]
22. Van Itallie CM, Anderson JM. Claudins and epithelial paracellular transport. Annu Rev Physiol 2006;68:403–29. [PubMed: 16460278]
23. Utech M, Bruwer M, Nusrat A. Tight junctions and cell-cell interactions. Methods Mol Biol 2006;341:185–95. [PubMed: 16799199]
24. Elias PM, Friend DS. The permeability barrier in mammalian epidermis. J Cell Biol 1975;65:180–91. [PubMed: 1127009]
25. Schluter H, Wepf R, Moll I, Franke WW. Sealing the live part of the skin: the integrated meshwork of desmosomes, tight junctions and curvilinear ridge structures in the cells of the uppermost granular layer of the human epidermis. Eur J Cell Biol 2004;83:655–65. [PubMed: 15679110]
26. Pummi K, Malminen M, Aho H, Karvonen SL, Peltonen J, Peltonen S. Epidermal tight junctions: ZO-1 and occludin are expressed in mature, developing, and affected skin and in vitro differentiating keratinocytes. J Invest Dermatol 2001;117:1050–8. [PubMed: 11710912]
27. Furuse M, Hata M, Furuse K, Yoshida Y, Haratake A, Sugitani Y, et al. Claudin-based tight junctions are crucial for the mammalian epidermal barrier: a lesson from claudin-1-deficient mice. J Cell Biol 2002;156:1099–111. [PubMed: 11889141]
28. Werner Y, Lindberg M. Transepidermal water loss in dry and clinically normal skin in patients with atopic dermatitis. Acta Derm Venereol 1985;65:102–5. [PubMed: 2408409]
29. Hon KL, Wong KY, Leung TF, Chow CM, Ng PC. Comparison of skin hydration evaluation sites and correlations among skin hydration, transepidermal water loss, SCORAD index, Nottingham Eczema Severity Score, and quality of life in patients with atopic dermatitis. Am J Clin Dermatol 2008;9:45–50. [PubMed: 18092843]
30. Nemoto-Hasebe I, Akiyama M, Nomura T, Sandilands A, McLean WH, Shimizu H. Clinical severity correlates with impaired barrier in filaggrin-related eczema. J Invest Dermatol 2009;129:682–9. [PubMed: 18818676]
31. Fallon PG, Sasaki T, Sandilands A, Campbell LE, Saunders SP, Mangan NE, et al. A homozygous frameshift mutation in the mouse Flg gene facilitates enhanced percutaneous allergen priming. Nat Genet 2009;41:602–8. [PubMed: 19349982]
32. Kubo A, Nagao K, Yokouchi M, Sasaki H, Amagai M. External antigen uptake by Langerhans cells with reorganization of epidermal tight junction barriers. J Exp Med 2009;206:2937–46. [PubMed: 19995951]
33. Klechevsky E, Morita R, Liu M, Cao Y, Coquery S, Thompson-Snipes L, et al. Functional specializations of human epidermal Langerhans cells and CD14+ dermal dendritic cells. Immunity 2008;29:497–510. [PubMed: 18789730]
34. Motta S, Monti M, Sesana S, Mellesi L, Ghidoni R, Caputo R. Abnormality of water barrier function in psoriasis. Role of ceramide fractions. Arch Dermatol 1994;130:452–6. [PubMed: 8166482]
35. de Cid R, Riveira-Munoz E, Zeeuwen PL, Robarge J, Liao W, Dannhauser EN, et al. Deletion of the late cornified envelope LCE3B and LCE3C genes as a susceptibility factor for psoriasis. Nat Genet 2009;41:211–5. [PubMed: 19169253]
36. Eichenfield LF. Consensus guidelines in diagnosis and treatment of atopic dermatitis. Allergy 2004;59 (Suppl 78):86–92. [PubMed: 15245365]
37. Cheadle C, Cho-Chung YS, Becker KG, Vawter MP. Application of z-score transformation to Affymetrix data. Appl Bioinformatics 2003;2:209–17. [PubMed: 15130792]
38. Nadon R, Shoemaker J. Statistical issues with microarrays: processing and analysis. Trends Genet 2002;18:265–71. [PubMed: 12047952]
39. Livak KJ, Schmittgen TD. Analysis of relative gene expression data using real-time quantitative PCR and the 2(-Delta Delta C(T)) Method. Methods 2001;25:402–8. [PubMed: 11846609]
40. Beck LA, Stellato C, Beall LD, Schall TJ, Leopold D, Bickel CA, et al. Detection of the chemokine RANTES and endothelial adhesion molecules in nasal polyps. J Allergy Clin Immunol 1996;98:766–80. [PubMed: 8876553]
41. Berry CA, Warnock DG, Rector FC Jr. Ion selectivity and proximal salt reabsorption. Am J Physiol 1978;235:F234–45. [PubMed: 696834]

NIH-PA Author Manuscript NIH-PA Author Manuscript NIH-PA Author Manuscript

42. Vidyasagar S, Ramakrishna BS. Effects of butyrate on active sodium and chloride transport in rat and rabbit distal colon. J Physiol 2002;539:163–73. [PubMed: 11850510]
43. Hallani M, Lynch JW, Barry PH. Characterization of calcium-activated chloride channels in patches excised from the dendritic knob of mammalian olfactory receptor neurons. J Membr Biol 1998;161:163–71. [PubMed: 9435272]
44. Poumay Y, Roland IH, Leclercq-Smekens M, Leloup R. Basal detachment of the epidermis using dispase: tissue spatial organization and fate of integrin alpha 6 beta 4 and hemidesmosomes. J Invest Dermatol 1994;102:111–7. [PubMed: 8288902]
45. Beck LA, Boguniewicz M, Hata T, Schneider LC, Hanifin J, Gallo R, et al. Phenotype of atopic dermatitis subjects with a history of eczema herpeticum. J Allergy Clin Immunol 2009;124:260–9. 9, e1–7. [PubMed: 19541356]
46. Hanifin JM, Thurston M, Omoto M, Cherill R, Tofte SJ, Graeber M. The eczema area and severity index (EASI): assessment of reliability in atopic dermatitis. EASI Evaluator Group. Exp Dermatol 2001;10:11–8. [PubMed: 11168575]
47. Carlson CS, Eberle MA, Rieder MJ, Yi Q, Kruglyak L, Nickerson DA. Selecting a maximally informative set of single-nucleotide polymorphisms for association analyses using linkage disequilibrium. Am J Hum Genet 2004;74:106–20. [PubMed: 14681826]
48. Howie BN, Carlson CS, Rieder MJ, Nickerson DA. Efficient selection of tagging single-nucleotide polymorphisms in multiple populations. Hum Genet 2006;120:58–68. [PubMed: 16680432]
49. Gabriel SB, Schaffner SF, Nguyen H, Moore JM, Roy J, Blumenstiel B, et al. The structure of haplotype blocks in the human genome. Science 2002;296:2225–9. [PubMed: 12029063]
50. Fan JB, Gunderson KL, Bibikova M, Yeakley JM, Chen J, Wickham Garcia E, et al. Illumina universal bead arrays. Methods Enzymol 2006;410:57–73. [PubMed: 16938546]
51. Gao PS, Rafaels NM, Hand T, Murray T, Boguniewicz M, Hata T, et al. Filaggrin mutations that confer risk of atopic dermatitis confer greater risk for eczema herpeticum. J Allergy Clin Immunol 2009;124:507–13. 13, e1–7. [PubMed: 19733298]
52. Sugiura H, Ebise H, Tazawa T, Tanaka K, Sugiura Y, Uehara M, et al. Large-scale DNA microarray analysis of atopic skin lesions shows overexpression of an epidermal differentiation gene cluster in the alternative pathway and lack of protective gene expression in the cornified envelope. Br J Dermatol 2005;152:146–9. [PubMed: 15656815]
53. Guttman-Yassky E, Suarez-Farinas M, Chiricozzi A, Nograles KE, Shemer A, Fuentes-Duculan J, et al. Broad defects in epidermal cornification in atopic dermatitis identified through genomic analysis. J Allergy Clin Immunol 2009;124:1235–44. e58. [PubMed: 20004782]
54. Brandner JM. Tight junctions and tight junction proteins in mammalian epidermis. Eur J Pharm Biopharm 2009;72:289–94. [PubMed: 18775491]
55. Brandner JM, Kief S, Grund C, Rendl M, Houdek P, Kuhn C, et al. Organization and formation of the tight junction system in human epidermis and cultured keratinocytes. Eur J Cell Biol 2002;81:253–63. [PubMed: 12067061]
56. Watson RE, Poddar R, Walker JM, McGuill I, Hoare LM, Griffiths CE, et al. Altered claudin expression is a feature of chronic plaque psoriasis. J Pathol 2007;212:450–8. [PubMed: 17582238]
57. Langbein L, Grund C, Kuhn C, Praetzel S, Kartenbeck J, Brandner JM, et al. Tight junctions and compositionally related junctional structures in mammalian stratified epithelia and cell cultures derived therefrom. Eur J Cell Biol 2002;81:419–35. [PubMed: 12234014]
58. Madara JL. Regulation of the movement of solutes across tight junctions. Annu Rev Physiol 1998;60:143–59. [PubMed: 9558458]
59. Schmitz H, Barmeyer C, Fromm M, Runkel N, Foss HD, Bentzel CJ, et al. Altered tight junction structure contributes to the impaired epithelial barrier function in ulcerative colitis. Gastroenterology 1999;116:301–9. [PubMed: 9922310]
60. Ussing HH, Zerahn K. Active transport of sodium as the source of electric current in the short-circuited isolated frog skin. Acta Physiol Scand 1951;23:110–27. [PubMed: 14868510]
61. van de Kerkhof EG, de Graaf IA, Groothuis GM. In vitro methods to study intestinal drug metabolism. Curr Drug Metab 2007;8:658–75. [PubMed: 17979654]
62. Wang W, Uzzau S, Goldblum SE, Fasano A. Human zonulin, a potential modulator of intestinal tight junctions. J Cell Sci 2000;113(Pt 24):4435–40. [PubMed: 11082037]

NIH-PA Author Manuscript NIH-PA Author Manuscript NIH-PA Author Manuscript

63. Yamamoto T, Saeki Y, Kurasawa M, Kuroda S, Arase S, Sasaki H. Effect of RNA interference of tight junction-related molecules on intercellular barrier function in cultured human keratinocytes. Arch Dermatol Res 2008;300:517–24. [PubMed: 18560860]
64. Yamamoto T, Kurasawa M, Hattori T, Maeda T, Nakano H, Sasaki H. Relationship between expression of tight junction-related molecules and perturbed epidermal barrier function in UVB-irradiated hairless mice. Arch Dermatol Res 2008;300:61–8. [PubMed: 18064478]
65. Tsukita S, Yamazaki Y, Katsuno T, Tamura A, Tsukita S. Tight junction-based epithelial microenvironment and cell proliferation. Oncogene 2008;27:6930–8. [PubMed: 19029935]
66. Lopardo T, Lo Iacono N, Marinari B, Giustizieri ML, Cyr DG, Merlo G, et al. Claudin-1 is a p63 target gene with a crucial role in epithelial development. PLoS One 2008;3:e2715. [PubMed: 18648642]
67. Kurasawa M, Kuroda S, Kida N, Murata M, Oba A, Yamamoto T, et al. Regulation of tight junction permeability by sodium caprate in human keratinocytes and reconstructed epidermis. Biochem Biophys Res Commun 2009;381:171–5. [PubMed: 19338770]
68. Kinugasa T, Sakaguchi T, Gu X, Reinecker HC. Claudins regulate the intestinal barrier in response to immune mediators. Gastroenterology 2000;118:1001–11. [PubMed: 10833473]
69. Tedelind S, Ericson LE, Karlsson JO, Nilsson M. Interferon-gamma down-regulates claudin-1 and impairs the epithelial barrier function in primary cultured human thyrocytes. Eur J Endocrinol 2003;149:215–21. [PubMed: 12943524]
70. Singh AB, Harris RC. Epidermal growth factor receptor activation differentially regulates claudin expression and enhances transepithelial resistance in Madin-Darby canine kidney cells. J Biol Chem 2004;279:3543–52. [PubMed: 14593119]
71. Kurahashi R, Hatano Y, Katagiri K. IL-4 suppresses the recovery of cutaneous permeability barrier functions in vivo. J Invest Dermatol 2008;128:1329–31. [PubMed: 17960173]
72. Sehra S, Yao Y, Howell MD, Nguyen ET, Kansas GS, Leung DY, et al. IL-4 regulates skin homeostasis and the predisposition toward allergic skin inflammation. J Immunol 184:3186–90. [PubMed: 20147633]
73. Hamid Q, Boguniewicz M, Leung DY. Differential in situ cytokine gene expression in acute versus chronic atopic dermatitis. J Clin Invest 1994;94:870–6. [PubMed: 8040343]
74. Peltonen S, Riehokainen J, Pummi K, Peltonen J. Tight junction components occludin, ZO-1, and claudin-1, -4 and -5 in active and healing psoriasis. Br J Dermatol 2007;156:466–72. [PubMed: 17300235]
75. Kirschner N, Poetzl C, von den Driesch P, Wladykowski E, Moll I, Behne MJ, et al. Alteration of tight junction proteins is an early event in psoriasis: putative involvement of proinflammatory cytokines. Am J Pathol 2009;175:1095–106. [PubMed: 19661441]
76. Itoh K, Kawasaki S, Kawamoto S, Seishima M, Chiba H, Michibata H, et al. Identification of differentially expressed genes in psoriasis using expression profiling approaches. Exp Dermatol 2005;14:667–74. [PubMed: 16098126]
77. Troy TC, Arabzadeh A, Lariviere NM, Enikanolaiye A, Turksen K. Dermatitis and aging-related barrier dysfunction in transgenic mice overexpressing an epidermal-targeted claudin 6 tail deletion mutant. PLoS One 2009;4:e7814. [PubMed: 19915705]
78. Hadj-Rabia S, Baala L, Vabres P, Hamel-Teillac D, Jacquemin E, Fabre M, et al. Claudin-1 gene mutations in neonatal sclerosing cholangitis associated with ichthyosis: a tight junction disease. Gastroenterology 2004;127:1386–90. [PubMed: 15521008]
79. Feldmeyer L, Huber M, Fellmann F, Beckmann JS, Frenk E, Hohl D. Confirmation of the origin of NISCH syndrome. Hum Mutat 2006;27:408–10. [PubMed: 16619213]
80. Zimmerli SC, Kerl K, Hadj-Rabia S, Hohl D, Hauser C. Human epidermal Langerhans cells express the tight junction protein claudin-1 and are present in human genetic claudin-1 deficiency (NISCH syndrome). Exp Dermatol 2008;17:20–3. [PubMed: 18095941]
81. Yuki T, Haratake A, Koishikawa H, Morita K, Miyachi Y, Inoue S. Tight junction proteins in keratinocytes: localization and contribution to barrier function. Exp Dermatol 2007;16:324–30. [PubMed: 17359339]

NIH-PA Author Manuscript

NIH-PA Author Manuscript

NIH-PA Author Manuscript

82. Tebbe B, Mankertz J, Schwarz C, Amasheh S, Fromm M, Assaf C, et al. Tight junction proteins: a novel class of integral membrane proteins. Expression in human epidermis and in HaCaT keratinocytes. Arch Dermatol Res 2002;294:14–8. [PubMed: 12071155]

83. Anderson JM, Van Itallie CM. Physiology and function of the tight junction. Cold Spring Harbor Perspect Biol 2009;1:a002584.

84. Meno K, Thorsted PB, Ipsen H, Kristensen O, Larsen JN, Spangfort MD, et al. The crystal structure of recombinant proDer p 1, a major house dust mite proteolytic allergen. J Immunol 2005;175:3835–45. [PubMed: 16148130]

85. Runswick S, Mitchell T, Davies P, Robinson C, Garrod DR. Pollen proteolytic enzymes degrade tight junctions. Respirology 2007;12:834–42. [PubMed: 17986111]

86. Groschwitz KR, Hogan SP. Intestinal barrier function: molecular regulation and disease pathogenesis. J Allergy Clin Immunol 2009;124:3–20. quiz 1–2. [PubMed: 19560575]

87. Arabzadeh A, Troy TC, Turksen K. Claudin expression modulations reflect an injury response in the murine epidermis. J Invest Dermatol 2008;128:237–40. [PubMed: 17625592]

88. French AD, Fiori JL, Camilli TC, Leotlela PD, O'Connell MP, Frank BP, et al. PKC and PKA phosphorylation affect the subcellular localization of claudin-1 in melanoma cells. Int J Med Sci 2009;6:93–101. [PubMed: 19305641]

89. McCall IC, Betanzos A, Weber DA, Nava P, Miller GW, Parkos CA. Effects of phenol on barrier function of a human intestinal epithelial cell line correlate with altered tight junction protein localization. Toxicol Appl Pharmacol 2009;241:61–70. [PubMed: 19679145]

90. Morar N, Willis-Owen SA, Moffatt MF, Cookson WO. The genetics of atopic dermatitis. J Allergy Clin Immunol 2006;118:24–34. quiz 5–6. [PubMed: 16815134]

NIH-PA Author Manuscript

NIH-PA Author Manuscript

NIH-PA Author Manuscript

A

	GENE	AD/NA Z ratio	AD/NA p value	PS/NA Z ratio	PS/NA p value
Gap Junctions	GJA1	-1.316	0.1312	0.176	0.9991
	GJA10	1.618	0.0011	-0.500	0.9950
	GJA12	-0.534	0.1885	-0.481	0.9954
	GJB5	0.392	0.4689	0.080	0.9992
	GJB4	-0.590	0.2838	-0.636	0.9928
	GJB2	5.175	0.0251	1.126	0.9882
Tight Junctions	CLDN1	-2.419	0.0013	-1.930	0.9774
	CLDN23	-3.160	0.0062	-0.591	0.9968
	TJP1	0.304	0.4465	-0.393	0.9952
	TJP3	-0.666	0.0605	0.550	0.8712
	TJP2	0.700	0.4888	0.836	0.9952
	OCLN	-1.136	0.0920	-1.389	0.9917
Differentiation Markers	SPRR1B	6.792	0.0208	1.367	0.9956
	SPRR1A	5.900	0.0600	1.180	0.9496
	SPRR2A	5.533	0.0118	1.020	0.9950
	SPRR2B	5.058	0.0866	0.031	0.9998
	IVL	0.556	0.7651	-1.842	0.9890
	TGM1	1.334	0.5398	-0.310	0.9984
	PPL	0.807	0.4825	0.351	0.9983

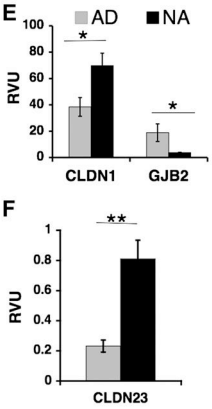

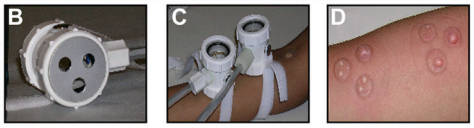

Figure 1. Intercellular junction proteins are dysregulated in AD subjects

(**A**) Z ratios from gene arrays performed on nonlesional epithelium (blister roofs, **B-D**), CLDN-1 and -23 were reduced, while the gap junction proteins, connexin-26 [*GJB2*] and connexin-62 [G*JA10*] were upregulated (**A**-Red). Genes indicative of de-differentiation were either unaffected or increased (**A**-Yellow). (**E, F)** Validation of the key genes in newly recruited AD/NA control samples (**P* = 0.03 & ***P* = 0.001).

NIH-PA Author Manuscript

NIH-PA Author Manuscript

NIH-PA Author Manuscript

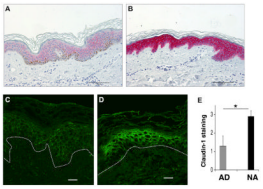

Figure 2. Claudin-1 expression is markedly reduced in AD epidermis

(**A**) Reduced claudin-1 immunoreactivity was noted in nonlesional AD skin (n = 11) compared to (**B**) NA (n = 12). Red indicates positive staining (Bar = 100 μm). Using a FITC-conjugated secondary antibody, claudin-1 had a membranous pattern in both (**C**) AD and (**D**) NA. The signal intensity was significantly reduced in (**C**) AD epidermis. Positive staining is indicated by green (Bar = 20 μm). The dotted line denotes the epidermal-dermal junction. (**E**) Semiquantitative scoring confirmed reduced epidermal expression of claudin-1 in AD (1.3 ± 0.3) compared to NA (2.9 ± 0.1; *P<0.0004).

NIH-PA Author Manuscript

NIH-PA Author Manuscript

NIH-PA Author Manuscript

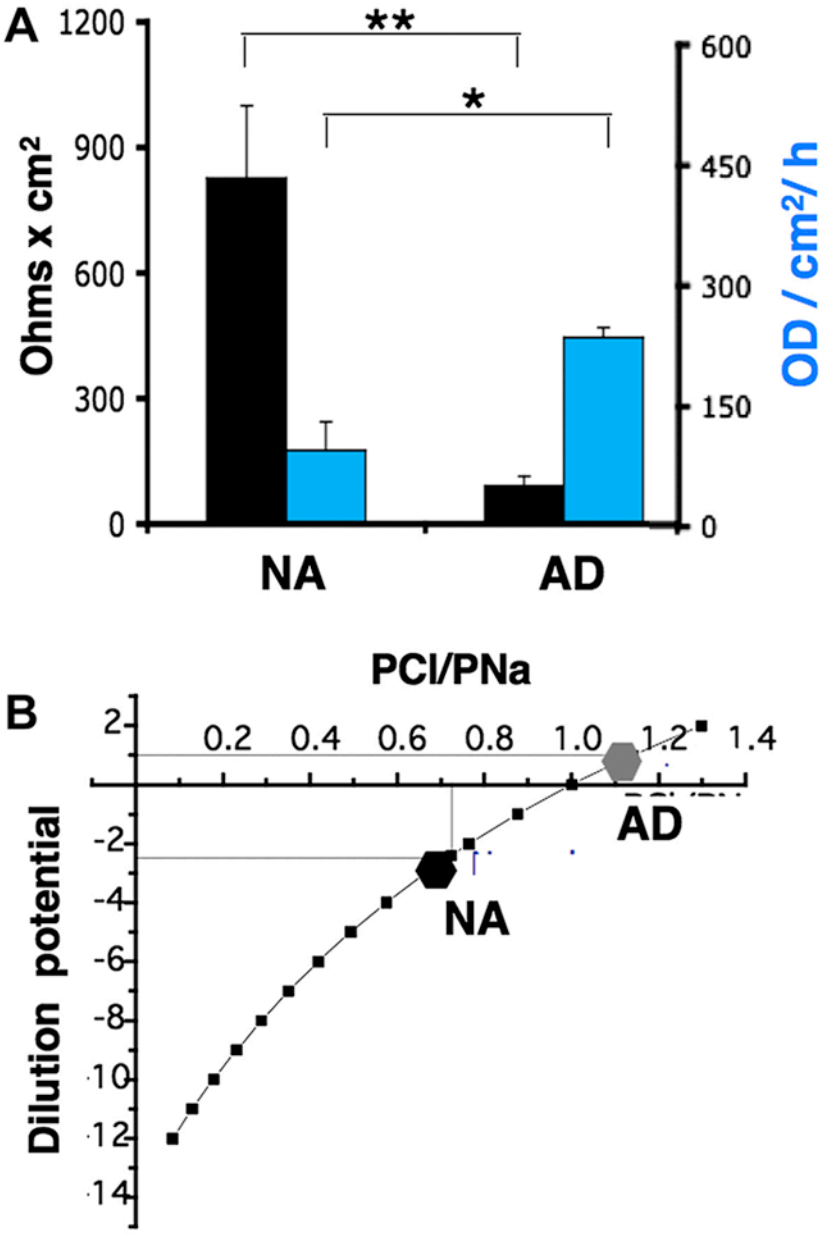

Figure 3. AD epidermis has altered bioelectric properties compared to NA

(**A**) Ussing chamber measurements reveal a markedly reduced resistance (92 ± 22.0 Ohms × cm^2; $n = 4$) in AD epithelium compared to NA (827 ± 173.3 Ohms × cm^2; $P = 0.01$; $n = 4$). This was reflected in an increased permeability to FITC-conjugated albumin in AD (445 ± 24.25 O.D./cm^2/h; $n = 4$) compared to NA (175± 68.37 O.D./cm^2/h; $P = 0.02$; $n = 4$). **(B)** Dilution potential studies noted the preservation of membrane selectivity in NA subjects, with Na^+ ions relatively more permeable than Cl^- (0.77 ± 0.03 fold PCl/PNa). In contrast, the selectivity was completely lost in AD epidermis (1.1 ± 0.02 fold PCl/PNa; $P = 0.001$; n = 3/group) and both ions were equally permeable.

NIH-PA Author Manuscript

NIH-PA Author Manuscript

NIH-PA Author Manuscript

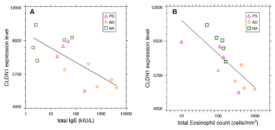

Figure 4. Claudin-1 expression from the gene arrays correlates with Th2 biomarkers

(**A**) The line represents the linear least square fit for $\log_2$ CLDN1 expression level vs. $\log_{10}$ total serum IgE (Pearson product-moment correlation coefficient $n = 14$; $r = -0.718$, $P = 0.0038$). (**B**) The plot of $\log_2$ CLDN1 expression level vs $\log_{10}$ total eosinophil count ($n = 14$; $r = -0.761$, $P = 0.0016$). The disease phenotypes (PS, AD, NA) are denoted by unique symbols.

NIH-PA Author Manuscript

NIH-PA Author Manuscript

NIH-PA Author Manuscript

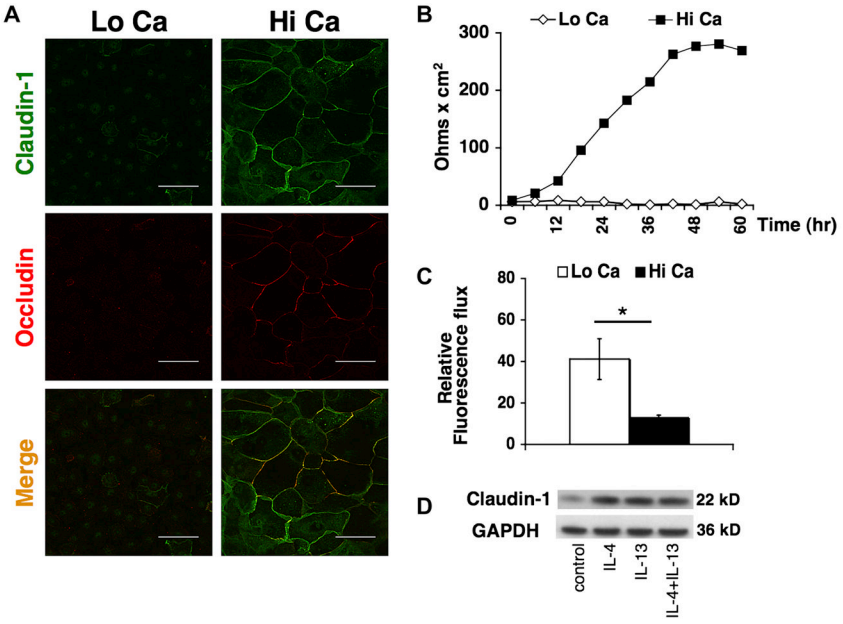

Figure 5. Claudin-1 colocalizes with other TJ proteins at the cell membrane in differentiated keratinocytes and this coincides with maximal TJ function

(A) In Ca^{2+}-differentiated keratinocytes (Hi Ca) claudin-1 (green) colocalizes with occludin (red) at the cell membrane. Bars = 50 μm. **(B)** TEER is only observed in differentiated PHK and peaks about 40h after the increase in Ca^{2+}. (Representative of n = 5). **(C)** Paracellular diffusion of 0.02% sodium fluorescein is markedly reduced in differentiated PHK (3.1 ± 0.6 fold; *P = 0.046; n = 3). **(D)** Western Blots show enhanced expression of claudin-1 when PHK were differentiated for 48h in presence of IL-4 (50 ng/ml) and IL-13 stimulation (50 ng/ml) or both cytokines (Representative of n = 3).

NIH-PA Author Manuscript

NIH-PA Author Manuscript

NIH-PA Author Manuscript

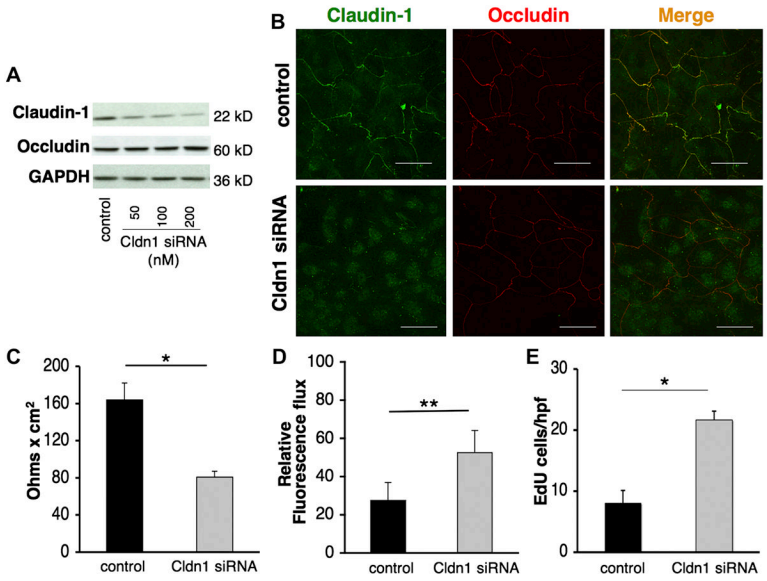

Figure 6. Claudin-1 silencing reduces TEER, increases paracellular permeability and enhances cell proliferation

(**A**) Western blots demonstrated a dose-dependent reduction of claudin-1 with CLDN1 siRNA (48h). No change was observed for occludin. (**B**) Immunostaining confirmed claudin-1 expression, but not occludin, was reduced in differentiated PHK following transfection with CLDN1 siRNA (Bars = 50 μm). (**C**) Claudin-1 knockdown significantly reduced TEER (control: 164 ± 18.2 and CLDN1 siRNA: 80.6 ± 6.4; **P* = 0.007; *n* = 4), (**D**) increased sodium fluorescein permeability (control: 27.6 ± 11.7 and CLDN1 siRNA: 52.5 ± 9.2; ***P* = 0.026; *n* = 4) and (**E**) enhanced cell proliferation as assessed by Click-iT™ EdU assay (***P* = 0.002; *n* = 3).

NIH-PA Author Manuscript

NIH-PA Author Manuscript

NIH-PA Author Manuscript

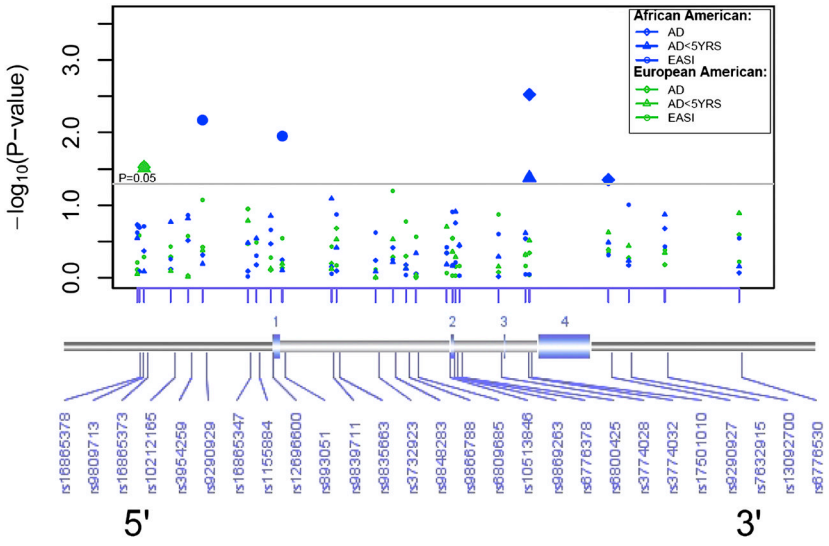

Figure 7. Evidence for *CLDN1* association with risk of atopic dermatitis (AD), early onset AD, and disease severity in two North American populations

The X-axis represents the physical position for each of 27 *CLDN1* SNPS shown in relationship to the exonic structure of the *CLDN1* gene on chromosome 3q.28-q29. The Y-axis denotes the association test result as -log (*P*-value) corresponding to representative symbols for each of the phenotypes. The standard cutoff for significance ($P = 0.05$) is shown as a horizontal solid line. Outcomes included risk of AD (diamond), early age of onset (<5 years; triangle) and the clinical scoring system called EASI (circle) in African American (AA; blue) and European American (EA; green) populations.

NIH-PA Author Manuscript

NIH-PA Author Manuscript

NIH-PA Author Manuscript

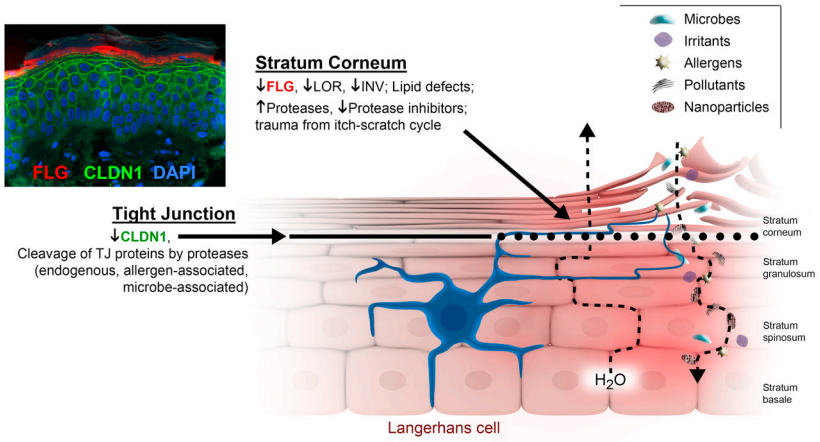

Figure 8.

Skin epithelium is uniquely armed with two barrier structures, the stratum corneum (SC) and tight junctions (TJ). The SC is the outermost structure consisting of multiple layers of enucleated keratinocytes called corneocytes. The SC barrier is maintained by the complex interaction of the cornified envelope, intracytoplasmic moisturizing factor(s) and a complex lipid mixture in the extracellular space[8]. TJ are located just below the SC at the level of the stratum granulosum (SG). The function of this structure can be accurately assessed by both resistance and permeability assays. In this paper we present evidence that this structure may be compromised in Atopic Dermatitis subjects and this may in part be due to reductions in claudin-1. These two barrier structures interact in a dynamic way to ensure that the skin maintains a formidable barrier. It is our premise that SC defects alone would not lead to the development or exacerbation of atopic dermatitis. We propose that a breach in both the SC and TJ would be required for sensitization to antigens/allergens, irritants, microbes, pollutants or possibly even nanoparticles. A recent study demonstrates that a temporary disruption in TJ results in the incorporation of Langerhans cell (LC) dendrites within a temporary TJ[32]. This extrusion of the LC dendrite would enable antigen uptake and processing by the LC and may confer some activation signals that would determine the immunologic fate of the APC-T cell interaction that follows. A fluorescence image of healthy human epidermis (left) demonstrates the expression patterns of two key players in AD pathogenesis, namely, FLG (red) and CLDN1 (green) and pictorially highlight the orientation of the two skin barrier components.

NIH-PA Author Manuscript

NIH-PA Author Manuscript

NIH-PA Author Manuscript

Table I

ADVN Genetics Study Demographics

Characteristic	European American		African American	
	AD	NA	AD	NA
Sample size	258	156	176	152
Males; N (%)	96 (37.2%)	63 (40.4%)	43 (24.4%)	77 (50.7%)
Age; mean (SD)	33.1 (18.5)	36.6 (13.2)	35.3 (12.5)	41.1 (10.3)
AD onset <5yrs; N (%)	178 (68.9%)	NA	91 (51.7%)	NA
Geometric mean IgE levels; (95% CI)	670.0 (502–895)	59.1 (48–111)	556.8 (425–729)	141.2 (113–299)
Geometric mean EASI[†]; (95% CI)	4.6 (3.9–5.4)	NA	4.0 (3.3–4.9)	NA
FLG Null Allele Carrier; N (%)	65 (25.2%)	9 (5.8%)	11 (6.2%)	2 (1.3%)

The following abbreviations are used: AD, atopic dermatitis; EASI, Eczema area and severity index; and NA, not applicable.

[†]EASI determined by the percentage of eczema area on a 7-point ordinal scale: 0 = <10%; 1 = 10%–29%; 3 = 30%–49%; 4 = 50%–69%; 5 = 70%–89%; and 6 = 90%–100